SUPPORTING INFORMATION FOR Spatial Coherence Manipulation on the Disorder-Engineered Statistical Photonic Platform

Leixin Liu[1], Wenwei Liu[2,], Fei Wang[3], Hua Cheng[2,*], Duk-Yong Choi[4], Jianguo Tian[2], Yangjian Cai[1,3,*], and Shuqi Chen[2,5,6,*]*

[1]Shandong Provincial Engineering and Technical Center of Light Manipulation & Shandong Provincial Key Laboratory of Optics and Photonic Device, School of Physics and Electronics, Shandong Normal University, Jinan 250014, China

[2]The Key Laboratory of Weak Light Nonlinear Photonics, Ministry of Education, Renewable Energy Conversion and Storage Center, School of Physics and TEDA Institute of Applied Physics, Nankai University, Tianjin 300071, China

[3]School of Physical Science and Technology, Soochow University, Suzhou 215006, China

[4]Laser Physics Centre, Research School of Physics, Australian National University, Canberra, ACT 2601, Australia

[5]The Collaborative Innovation Center of Extreme Optics, Shanxi University, Taiyuan, Shanxi 030006, China.

[6]The Collaborative Innovation Center of Light Manipulations and Applications, Shandong Normal University, Jinan 250358, China

Corresponding Authors

*E-mail: wliu@nankai.edu.cn.

*E-mail: hcheng@nankai.edu.cn.

*E-mail: yangjiancai@suda.edu.cn.

*E-mail: schen@nankai.edu.cn.

S1. SAMPLE FABRICATION

The dielectric statistical TiO_2 metasurfaces were fabricated on a cleaned fused silica substrate. Firstly, a layer of 550 nm electron-beam resist (ZEP 520A from Zeon) was spin-coated on the substrate, then baked on a hot plate at 180 °C for 1 min. To prevent charging during electron-beam writing, a thin layer of the E-spacer 300Z (Showa Denko) was coated on the resist. The nanostructures were defined by electron-beam lithography (Raith150) at 30 kV with 20-pA current and 80 $\mu C/cm^2$ dose, followed by development in n-amyl acetate solvent at room temperature for 60 seconds. Conformal TiO_2 layer with a thickness of approximately 70 nm was deposited by an atomic layer deposition system (Picosun) using titanium tetrachloride and H_2O as precursors at a reactor temperature of 130 °C. Subsequently, CHF_3 plasma in an inductively coupled plasma-reactive ion etching (ICP-RIE, Oxford system 100) was performed to blank- etch the TiO_2 layer until the ZEP 520A resist was exposed. Here the etching conditions were 20 sccm of CHF_3 at 50 W bias power/500 W induction power at an operating pressure of 10 mTorr, which resulted in a TiO_2 etching rate of ~20 nm per minute. Finally, O_2 plasma with small addition of CHF_3 was used to fully remove the remaining ZEP resist.

S2. MEASUREMENT PROCEDURE

The laser beam collimated by a fiber collimator from a supercontinuous laser (NKT SuperKEXR-20) passed through a polarizer and a quarter-wave plate to obtain a left-handed circularly polarized light. Then, a 4*f*-system (L1 and L2 with focal lengths

of 30 mm and 100 mm) was used to obtain an expanded collimated laser beam. To match the beam width with the size of each region of the metasurface, another lens L3 (focal length of 150 mm) was used to focus the beam to a spot size of 30 μm. The focused beam was incident onto the statistical metasurface, and the movement of the statistical metasurface along the *x*-direction was controlled by an electric translation stage (e-X). Before measurement, the statistical metasurface and translation stage (e-X) need to be calibrated by a three-dimensional translation stage and a rotating stage. The coherence of the beam has been changed when passing through the statistical metasurface, and the instantaneous intensity of the transmitted light was captured by an imaging system, which contains an objective (Obj1), a tube lens (TL), and a CCD camera. Another quarter-wave plate and polarizer pair were employed to filter the right-handed circularly polarized component of the signals. In the experiments, we measured the light distributions at a plane with a distance of 120 μm away from the metasurface. The convergence of the measured coherence can be found in Supplemental Figs. S3 and S4.

S3. DESIGN PRINCIPLE OF PHASE DISTRIBUTIONS OF THE STATISTICAL METASURFACES

The concept of statistical metasurface is introduced to manipulate the spatial coherence of the beams, by loading a random phase distribution onto the wavefront, and performing a scanning process to obtain a series of instantaneous intensities that can be statistically analyzed. We design the phase fluctuation range (PFR) of $[\pi - i\pi,$

π + iπ], where $i \in [0,1]$ is a parameter for the phase design. The phase φ is linearly and uniformly distributed in PFR with φ = π + *rand*(2iπ), where the *rand*(2iπ) function returns a uniformly distributed random real number in the interval [–iπ, iπ]. The probability density of the phase distribution can be calculated through:

$$P(\varphi)=\begin{cases}0, & \varphi<(1-i)\pi \\ \dfrac{1}{2i\pi}, & (1-i)\pi\le\varphi\le(1+i)\pi \\ 0, & \varphi>(1+i)\pi\end{cases}, \quad i=\{0, 0.2, 0.4, 0.6, 0.8, 1\}\ . \quad (1)$$

Generally, the randomly distributed phase can be arbitrarily designed, leading to partially coherent beams with different coherent lengths. Specifically, we realize a statistical metasurface of 6 regions with different uniform phase distributions for 6 parameters in Eq. (1), and the corresponding $\Delta\varphi$ is 0, 0.4π, 0.8π, 1.2π, 1.6π, 2π, respectively.

S4. NUMERICAL SIMULATION OF THE TRANSMITTED BEAM FROM THE STATISTICAL METASURFACE

To verify the convergence of the measured degree of coherence (DOC) of the generated beams, the experimental process is simulated through the commercial software MATLAB. The electric fields distribution of the source field beam is defined as:

$$E(\xi,\eta)=A_j\exp(-i\varphi), \quad (2)$$

where A_j and φ denote the amplitude and phase of the electric fields of the light transmitting from the statistical metasurface. The source intensity with transverse coordinates (ξ , η) is defined by a function I_0 (ξ , η), which locates at the plane of the

statistical metasurface. The source fields propagate to the observation plane with transverse coordinates (x_n , y_n). Such propagation can be calculated through an ABCD optical system:

$$E\left(x_n, y_n\right) = \frac{ik}{2\pi B}\exp\left[\frac{ikD\left(x_n^2 + y_n^2\right)}{2B}\right]\iint E\left(\xi,\eta\right) \times\exp\left[\frac{ikA}{2B}\left(\xi^2+\eta^2\right)\right]\exp\left[\left(-\frac{ik}{B}\xi x_n - \frac{ik}{B}\eta y_n\right)\right]d\xi d\eta \quad . \tag{3}$$

Generally, it is challenging to find an analytical solution of Eq. (3). To evaluate the output modes, we define a new function *f*:

$$f\left(\xi,\eta\right) = E\left(\xi,\eta\right)\exp\left[\frac{ikA}{2B}\left(\xi^2+\eta^2\right)\right]. \tag{4}$$

Substituting Eq. (4) into Eq. (3), the propagation of the source fields can be evaluated using the FFT algorithm, i.e.,

$$E\left(x_n, y_n, z_n\right) = \frac{ik}{2\pi B}\exp\left[\frac{ikD\left(x_n^2 + y_n^2\right)}{2B}\right]F\left\{f\left(\xi,\eta\right)\right\}, \tag{5}$$

where the operator *F* is the Fourier transform operator. Therefore, the *i*th instantaneous intensity of the partially coherent beams in the output plane can be expressed as:

$$I_i\left(x_n, y_n, z_n\right) = \left|E_i\left(x_n, y_n, z_n\right)\right|^2 . \tag{6}$$

To implement the statistical ensemble average, *K* instantaneous intensities are further generated with varied phase distributions in the source plane due to the random process, and the average light intensity in the observation plane can be written as:

$$I\left(x_n, y_n, z_n\right) = \frac{1}{K}\sum_{i=1}^{K}\left|E_i\left(x_n, y_n, z_n\right)\right|^2 . \tag{7}$$

Moreover, the coherence of the generated beams can be calculated through:

$$\mu\left(x_n, y_n, z_n\right) = \frac{\sum_{i=1}^{K}\left[E\left(\boldsymbol{\rho}_1, z_n\right)\right]^* E\left(\boldsymbol{\rho}_2, z_n\right)}{\sqrt{I\left(\boldsymbol{\rho}_1, z_n\right) I\left(\boldsymbol{\rho}_2, z_n\right)}}, \tag{8}$$

where $\boldsymbol{\rho}_1$ and $\boldsymbol{\rho}_2$ are two position vectors in the observation plane. Equations (2)-(8) provide a convenient way to numerically study the intensity and the coherence of the generated beams in the ABCD optical system.

An illustration of the numerical simulation process of the beam generated from the statistical metasurface is shown in Fig. S2. The metasurface located at the source plane can generate a temporal phase distributions within a limited PFR. The transmitted light was captured by an imaging system to record the light distributions with a total number of K. By moving the imaging system along the z direction, the instantaneous intensity distributions at different distances z_1, z_2, …, z_n are obtained and the coherent lengths of the beams at the corresponding plane are calculated, respectively. Generally, the coherent length of the light gradually increases as the transmission distance z_n increases until the coherence of the light converges.

We also simulated the experimental process considering the devices parameters in our experimental setup. We chose a series of statistical metasurfaces whose phase randomly and uniformly covers the PFR with [0, 2π] to simulate the partially coherent light at different transmission distances. According to Eq. (8), we simulated the coherent lengths of the generated beams at different transmission distances (Fig. S3), which meet well with the measured ones. The theoretical and the experimental results with the PFR of [0, 2π] show that the measured coherent length will converge when the transmission distance is large enough. The experimental results for other PFR

setups at different transmission distances also verify the convergence of the DOC as shown in Fig. S4.

SUPPORTING FIGURES

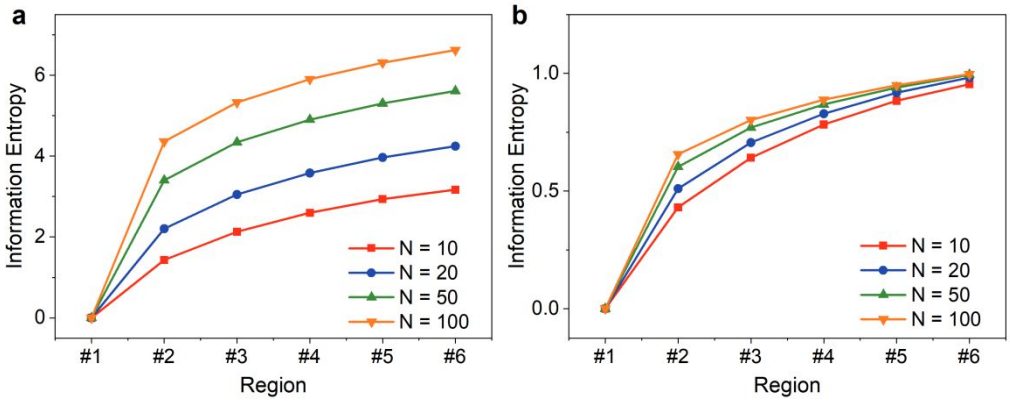

Figure S1. Calculated information entropy of the designed statistical metasurface with different definitions. The information entropy is defined as (a) $-\sum p \log_2 p$ and (b) $-\sum p \log_N p$ for uniformly N-divided phase in the phase interval of 0–2π. The difference between the two definitions is different unit systems.

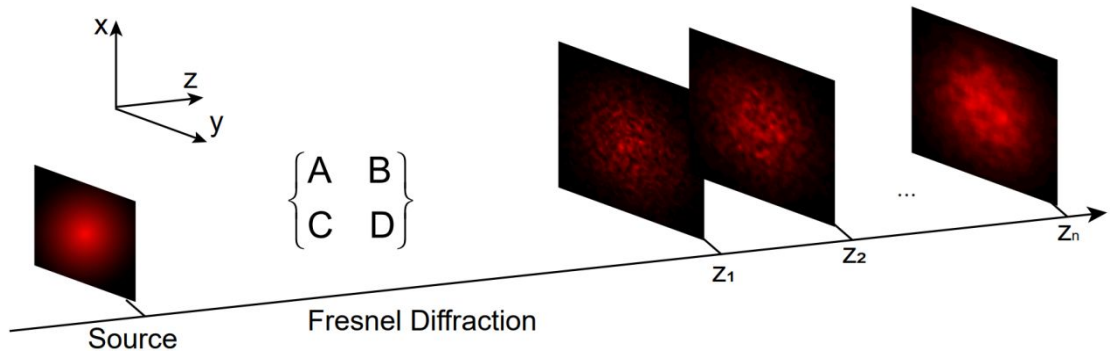

Figure S2. Schematic of the propagation of the generated partially coherent beams captured in different *z* locations.

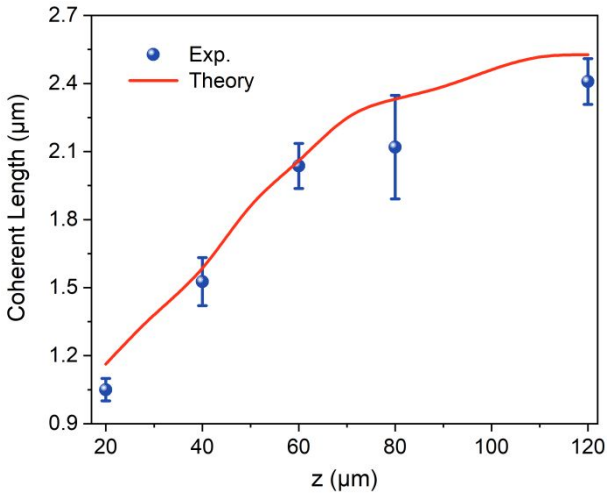

Figure S3. Theoretical and experimental results of coherent lengths at different transmission distances when the PFR covers [0, 2π]. The error bar indicates the statistical fluctuation induced by the incomplete sets of cut-lines and measurements.

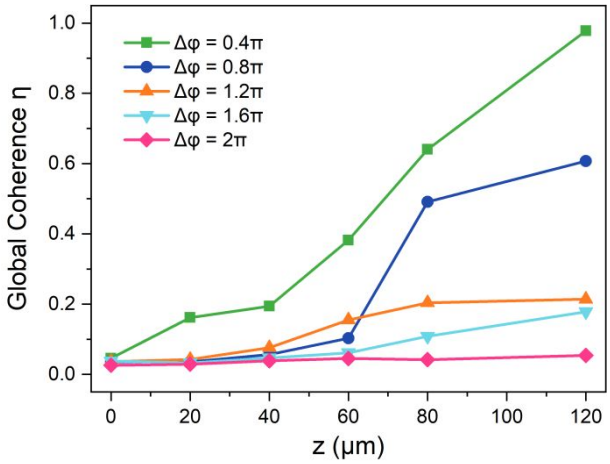

Figure S4. The global coherence of each phase distribution at different distances from the statistical metasurface. The experimental results show that the global coherence of each phase distribution increases with the increase of distance from the metasurface and finally tends to converge. It is conformed with the van Cittert-Zernike theorem[1].

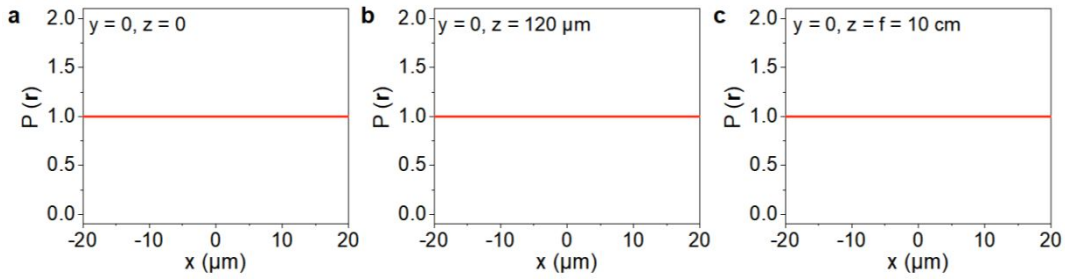

Figure S5. DOP of the output beams at the (a) z = 0, (b) z =120 μm, (c) z = f = 10 cm cut-planes along the y = 0 cut-line. The DOP of the generated beam at the two cut-planes is uniform and equals to one.

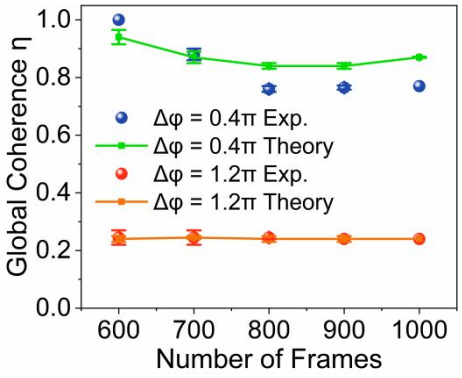

Figure S6. The theoretical and experimental global coherence as a function of different numbers of the captured frames. The Global coherence gradually converges when the number of frames reaches more than 800 and 600 for $\Delta\varphi = 0.4\pi$ and 1.2π, respectively.

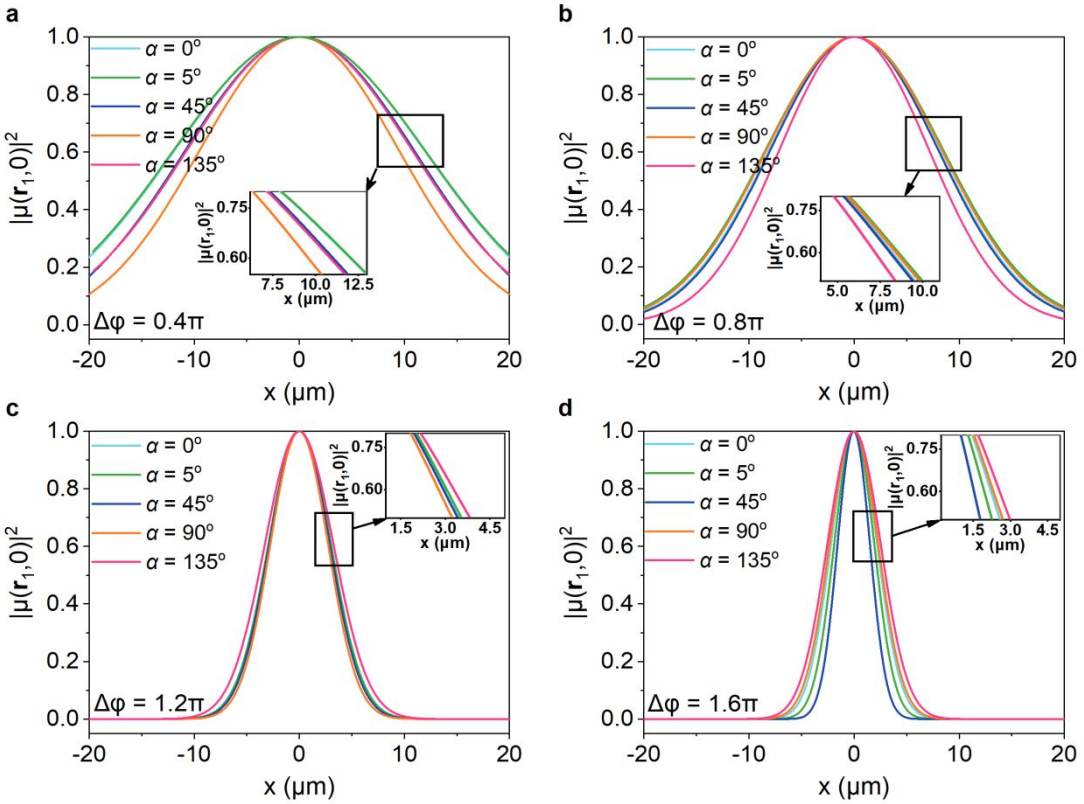

Figure S7. Gaussian curve-fitting of $|\mu(\mathbf{r}_1, 0)|^2$ for (a) $\Delta\varphi = 0.4\pi$, (b) 0.8π, (c) 1.2π and (d) 1.6π for different cut-line orientation angles α which is defined as the intersection with the $+y$ direction shown in Figure 4b. Inset: zoom in the influence of α. The coherence distributions for different angles with limited fluctuation results from the fabrication imperfection and are statistically analyzed to obtain the DOC.

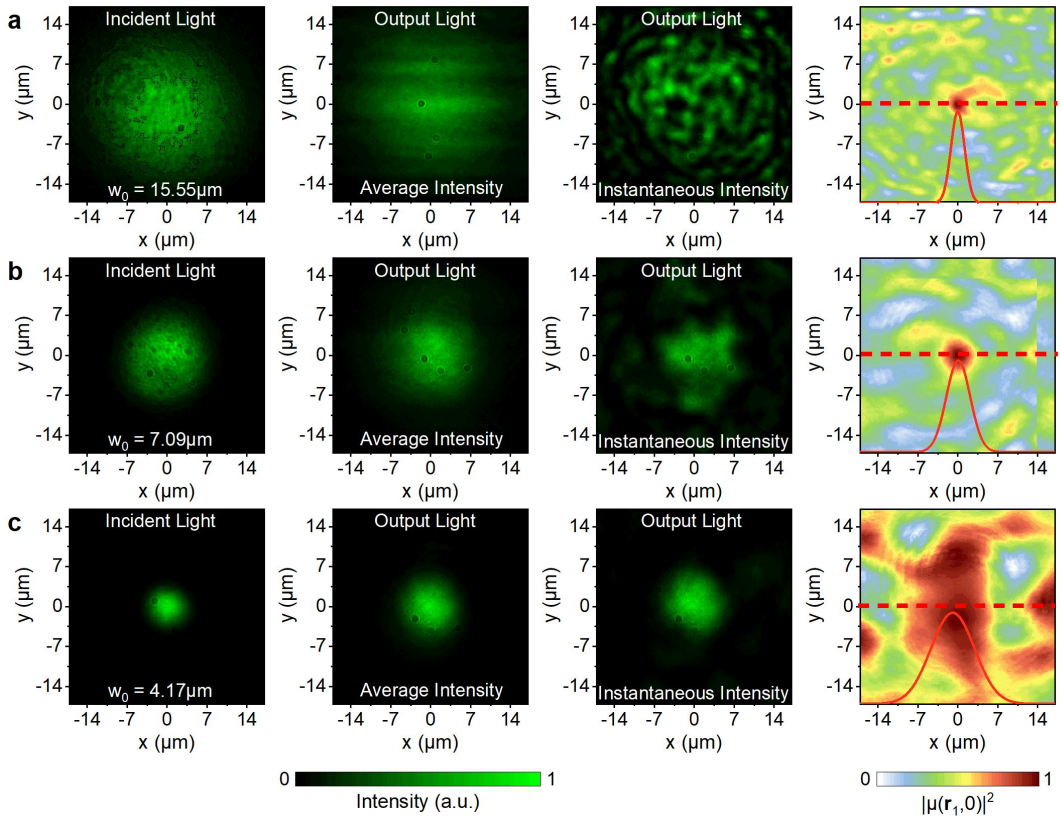

Figure S8. Experimental results of the spatial coherence manipulation by controlling the beam width ω_0 of the incident light. (a) $w_0 = 15.55$ μm, (b) $w_0 = 7.09$ μm, (c) $w_0 = 4.17$ μm (first column) are focused onto the statistical metasurface with 0-2π PFR, the average intensity distributions (second column) and instantaneous intensity distributions (third column) of the output light are respectively captured by the CCD camera when scanning the metasurface. The average intensity distributions can be calculated by averaging the ×1000 measured instantaneous intensity distributions or directly obtained by the CCD camera when scanning speed is quickly enough or the exposure time of CCD is long enough. The fourth column shows the Experimental distributions of $|\mu(\mathbf{r}_1, 0)|^2$ with corresponding incident light beam width and the Gaussian curve-fitting along the $x = 0$ cut-lines. The experimental results indicate the coherence of the beam increasing with the incident beam width decreased.

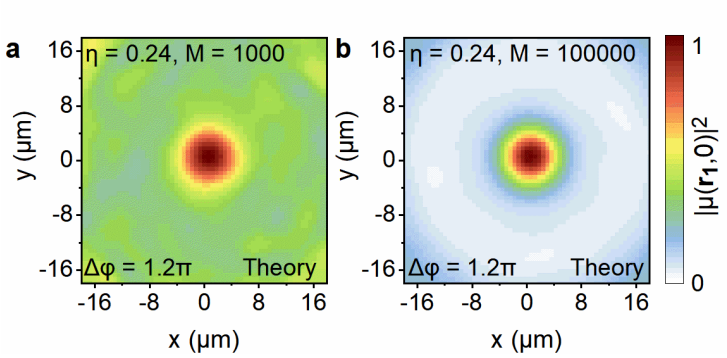

Figure S9. Calculated distributions of $|\mu(\mathbf{r}_1, 0)|^2$ for $\Delta\varphi = 1.2\pi$ at the z = 120 μm cut-plane with different numbers of frames with (a) M=1000, (b) M = 100000.

SUPPORTING VIDEO LEGENDS

Supplemental Video 1 | Measured instantaneous intensity distributions for different PFRs while scanning. The video shows the continuous instantaneous intensity distributions for the 6 regions of the statistical metasurface. When the scanning speed is fast enough, the intensity distribution of the generated beam will be homogeneous captured by the CCD camera in the experiment.

SUPPORTING REFERENCE

1 Zernike, F. The concept of degree of coherence and its application to optical problems. *Physica* **1938**, 5, 785.